Mono-Koto Interaction Produces Sensitivity

Tani, Iori

博　士　論　文

Mono-Koto Interaction Produces Sensitivity

（感覚をつくるものとことの相互作用）

平成 26 年 1 月

神戸大学 大学院理学研究科 地球惑星科学専攻

谷　伊織

DOCTORAL DISSERTATION

Mono-Koto Interaction Produces Sensitivity

Iori TANI

January 2014

Abstract

The origin of our sensitivity is not understood sufficiently. In the background of this problem, there is a conflict between "Mono" and "Koto". Our sensitivity have been regarded as "Koto" that can not be described by aggregation of "Mono". I propose another perspective that gives us constructive approaches to this exclusive dichotomy. "Sensitivity" has characteristics of both "Mono" and "Koto" , and therefore, it is a product of an interaction between information processes based on "Mono" and "Koto".

To verify this viewpoint, I conducted an experiment using bio-computer consists of true slime mould *Physarum polycephalum* and demonstrated our sensitivity can be emulated by bio-computer. The plasmodium of *P. polycephalum* is often used in the implementation of non-linear computation to solve optimization problems, and this organismal feature was not used in this analysis to compute sensitivity in humans.

In this dissertation, I focused on the Kanizsa illusion, which is a well-known visual illusion, because visual illusion is considered as a by-product of our information processes including interaction of lower("Mono") and higher("Koto") order information. I demonstrated that the network pattern mimicking the Kanizsa illusory contour can be reproduced by an asynchronous automata-fashioned model of the slime mould and by the foraging real plasmodia of *P. polycephalum*. Because the protoplasm of the plasmodium is transported depending on both local and global computation, it may connect differentiation("Mono")-integration("Koto") processes. In this sense, the idea of perception and sensitivity can be extended.

Contents

Chapter 1

Introduction

1.1 "Mono" and "Koto"

I begin this work from definitions of the meanings that were indicated by the words "Mono (もの)" and "Koto (こと)" to clarify the point of my argument. As discussed afterwards, "Mono" and "Koto" are appearance of individual phenomena rather than the fixed properties of them. In Japanese language, We usually point out an individual by the word "Mono". And, we call a situation or conditions "Koto". But here, I use the words "Mono" to express a more extended meaning. Because of this, the meaning of "Koto" will become more restricted than ordinary one.

Ludwig Wittgenstein distinguished "facts" and "things" exactly. He said in his first work as following, "The world is the totality of facts, not of things." He also said, "The world divides into facts."[35] What did he mean by these propositions? According to Noya[36], Wittgenstein called the cases such as "There is a red book on a black desk." "facts". In contrast, the individual components of the "fact", for example "book", "desk", "black" and "red" are called "things". i.e. "Facts" were interpreted as specific relationships between the "things" and these "things" are provided by deconstructing the

"facts". Wittgenstein attempted to begin his philosophical argument with the level of "facts", not of "things".

We think this type of distinction that a "facts" are particular combination of "things' is highly reasonable ordinary, especially in scientific sense. Neverthless, it is premature to associate "Mono" with "things" and "Koto" with "facts". It is necessary to notice that Wittgenstein mentioned another level of distinction.

> What can be said at all can be said clearly; and whereof one
> cannot speak thereof one must be silent. [35]

I do not discuss what did Wittgenstein consider that can be said or not here. But, this separation is more serious than the gap between "facts" and "things". Wittgenstein suggested in these words the existence of what cannot be said and therefore cannot nothing do but be shown[36].

For the present, I use the word "Mono" to indicate "what one can said". In other words, what we have an appropriate language to describe them are called "Mono". "Mono"s have a clear boundary and unity. And therefore, we can distinguish from others and operate freely. In this viewpoint, the proposition such above "There is a red book on a black desk." can be regard as "Mono" because this sentence has a clear boundary and unity in a particular context. Therefore, a finite combination of "Mono"s can also be considered as "Mono".

In contrast, "Koto" cannot be divided into the aggregation of "Mono" and the boundary of "Koto" is undecided. In this sense, "Koto" can not be speak. "Paradox of the heap" gives a typical example of "Koto". This paradox says that the heap is not a simple aggregation of grains of sands, and therefore it is a "Koto". We can only say "There is a heap." or "It is a heap.", but we cannot speak about "What is a heap?" or "Why is this a

heap?" exactly.

It is necessary to notice that "Mono" and "Koto" are appearance or interpretation of phenomena depending on the context, not static state of them. Actually, we can regard the heap as an aggregation of grains of sand. And, we can also regard the heap as a "Mono" compose another "Koto". In science study, "Koto" have been analyzed by resolving into "Mono"s. However, there are many cases that such analyses do not work effectively in biological phenomena, especially in brain activities concern with our consciousness.

1.2 The "propositional" and "phenomenal" components of experiences

Nicholas Humphrey, a Brithsh ethologist or philosopher, divided the components of our experiences into "propositional" and "phenomenal" one [13]. "Propositional" components are representation of what is going on. They are also called perception. On the other hand, "phenomenal" components indicate our feeling including "qualia". In other words, "propositional" corresponds to "objective" and "phenomenal" corresponds to "subjective"

Humphrey negated the existence of causality between perception and feeling according to his observation about blind sight. Blind sight is a rare disease caused by structural disorder of brain. The patients of blind sight report that they do not have any visual qualia, that is they think they must be totally blind. Nevertheless, there are cases that they are able to avoid the obstacle in front of them or describe objects in a room when they are asked, just like they have complete visual information.

Humphrey insists that these symptoms suggest that our perception and feeling are processed in parallel. We usually think that our perception is caused by particular feeling. That is to say, we usually think that our feeling

or qualia produce our perception. But, the blind sight patients can percept without feeling. He explains the origins of these two aspects of consciousness by historical processes of evolution.

Here, There is a question to what degree these processes are parallel. If these are completely distinguished, in other words, if there is no interaction between the perception and feeling, we would not be able to have any emotion. Because, our emotion includes the "perception about our feeling" and "feeling about our perception". Therefore, there is necessity of the interaction. Humphrey reported the patient do not try to use their ability voluntarily and they are not impressed by their ability. This report suggests they lost particular conscious activity because they do not have feeling. I call these emotion that is provided by the interaction between perception and feeling "sensitivity".

"Sensitivity" has the characteristics of both "Mono" and "Koto" because it is provided by interaction of them. Here, another question occurs. That is to say, nevertheless they have different characteristics respectively, what permits the interaction of perception which is "Mono" and feeling which is "Koto". I think the processes of perception and feeling are not completely parallel and there are particular functionality that confuse them in the same level.

1.3   Interaction between "Mono" and "Koto"

As discussed above, phenomena have an ambiguity that they are not decided whether "Mono" or "Koto". This ambiguity regard "Mono" and "Koto" in the same level and permits their interaction. I think we use this ambiguity positively in functional level of brain activity because it allows information contraction in process level.

In generally, we process huge amount of information that are obtained by sense organs. To use the information effectively, we have to contract them and select important one from large information flow. Therefore, It is not effective to regard all information as "Mono". To avoid this, "Mono" are unified to "Koto".

For example, our visual information have huge volume and we usually use this information mainly. There is a conflict of "Mono" and "Koto" here such as neurons v.s. consciousness. The information of stimuli that are received by photoreceptor cell are considered as "Mono", On the other hand, a total field of vision that consists of local stimuli are considered as "Koto". We usually do not use "Mono" information such as "There is a gradient of stimuli here" directly. In stead of them, we coordinate them and create "Koto" information such as "There is a border of something." and so on. This ability has highly important role in our speedy information processes. But, this provide a by-product to our consciousness, that is visual illusion. I consider particular visual illusions are results of the information integration that contract lower-order information.

In this dissertation, I focused on the Kanizsa illusion, which is a well-known visual illusion resulting from the differentiation-integration of the visual field, and compared the illusion with the adaptive network in the plasmodium of *Physarum polycephalum*. The differentiation corresponds to "Mono" based process, and the integration corresponds to "Koto" based one. I demonstrated that the network pattern mimicking the Kanizsa illusion can be produced by an asynchronous automata-fashioned model of the foraging slime mould and by the real plasmodia of *P. polycephalum*. Because the protoplasm of the plasmodium is transported depending on both local and global computation, it may contain differentiation-integration processes. Therefore,

the plasmodia can creates some "sensitivity". In this sense, we can extend the idea of sensitivity.

Chapter 2

Production of Sensitivity: Kanizsa illusory contour appear in the network pattern of true slime mould *Physarum* plasmodium

2.1 Introduction

A true slime mould, *Physarum polycephalum* (order Physarales, class Myxomycetes, subclass Myxogastromycetidae) has been used as a model organism to investigate biologically motivated unconventional computing because the plasmodium of *Physarum* can solve various theoretical graph problems, including a Steiner tree, Spanning tree [1], maze [19, 20] and Voronoi diagram [26, 28]. The plasmodium can also perform logical computing [34, 2] and create an optimal adaptive network [33, 11].

These computations, which produce particular patterns in relation to the input stimulus, were previously distinguished from psychological reactions such as sensation and emotion; however, sensation and emotion are also

9

considered higher-order computations in which pattern formation is applied to the deviation and/or representation of the input stimulus [3, 25]. In this sense, it is possible to say that even an amoeboid animal can feel something [13]. Whereas the retreat of the marginal front of the amoeba away from a repellant stimulus can be considered a lower-order computation, the reaction to a particular transportation of protoplasm from one margin to the other areas can be regarded as a sensation or a higher-order computation relative to the lower-order one.

When the plasmodium of *Physarum* forages in an environment, the extension or retreat of a local area can lead to the elongation and/or shortening of the tubular network and vice versa. This phenomenon reveals that a lower-order computation can lead to a higher-order computation and vice versa. The synthesis of local and global information propagation can result in a reaction to an external stimulus coupled with a higher-order computation, which might be considered "perception". This extended perception gives rise to the idea that the plasmodium can emulate and/or compute the perception of a human.

The visual perception of humans is not a simple local reaction to an optical stimulus, such as with a camera. Computing an optical stimulus is not only a local computation but also a global computation, and the local reaction to the optical stimulus can be modified depending on the global propagation of information. A visual illusion is one of the most intriguing examples of visual perception that results from the synthesis of local and global computation. In the Müller-Lyer illusion, the apparent length of a local pattern can be shortened or extended depending on its surrounding pattern [18, 12]. In the aforementioned sense, biologically motivated computing can reveal visual illusion in terms of the analogy at the phenomenological and mecha-

nistic levels. It was previously demonstrated that the distribution of foraging ants attracted to the honey dew along a Müller-Lyer diagram can reveal a Müller-Lyer illusion, wherein the ants in an attractive field can be compared to the neurons in a visual field [25]. Not only ants but also the plasmodium of *Physarum* can emulate various visual illusions because the plasmodium integrates lower- and higher-order computations. In this study, I focus on a particular visual illusion, Kanizsa illusory contours.

Kanizsa illusory contours are subjective shapes induced from local pac-man elements [15]. According to Gestalt psychology, human vision is sensitive not to the input stimulus per se but to the relative values of input signals [16]. This idea, when theoretically enforced [24], explains that the Kanizsa illusion is triggered by the relative contrast in the Kanizsa diagram, developed by contour completion and finally completed by filling in [22].

Although the process of contour completion was first explained using a simple collinearity-based model [7, 8], the disappearance of illusion cannot be explained by this model when the pac-man elements in the Kanizsa figure are replaced by crosses. The simple filling-in is unable to explain the perceived brightness and/or occlusion of the central area of the Kanizsa illusory contours, as noted by Coren[5]. To resolve these problems, a differentiation-integration approach is employed by some models [6]. The edge of the bright area is detected by differentiation, and the contrast of the pac-man is also preserved in a memory. Through integration, this information creates a line connecting the pac-men, the brighter surface in the central area and the relative depth featuring the occlusion cues [17]. By introducing a particular mechanism in which the local elongations of contours interact and are cancelled, the disappearance of the illusion for a particular variation of a Kanizsa figure can be explained.
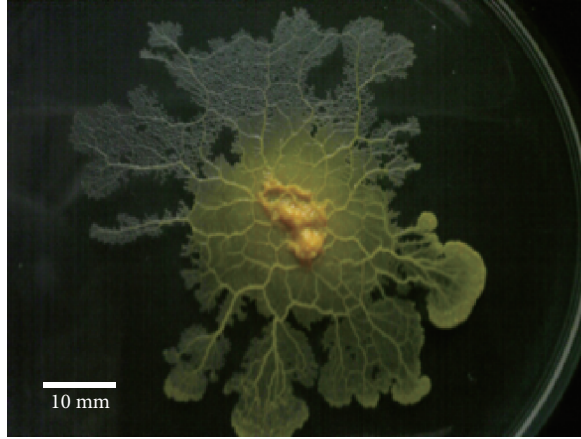
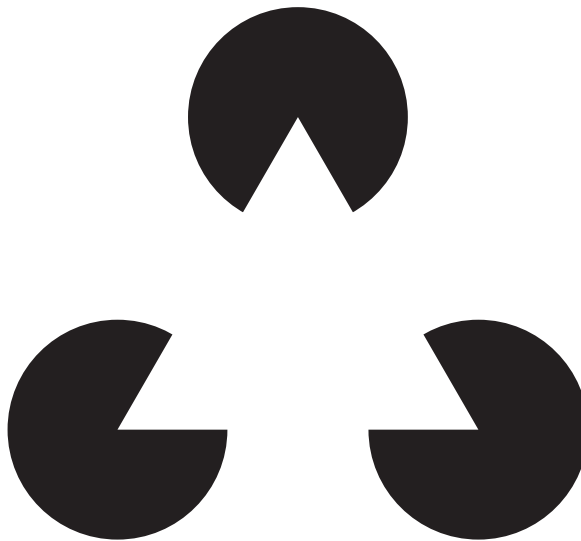Figure 2.1: The plasmodium of true slime mould *Physarum polycephalum*

Figure 2.2: Kanizsa diagram

When the plasmodium of the *Physarum* is considered, the Kanizsa illusory contours might be emulated by a real foraging plasmodium. An asynchronously updated automata-fashioned model for the plasmodium of the *Physarum* was proposed previously [10, 9, 11, 21]. This model can mimic amoebic motions, adaptive networks and growth patterns in unstimulated environments of the plasmodium of *Physarum*. Because this model is based on the local detection of the environmental stimulus and the asynchronous transportation of protoplasm, the model can embed the synthesis of the differentiation-integration process. In this sense, the model and/or the real plasmodium of *Physarum* can connect separated pac-men by a tubular structure, which reveals an illusory contour. We ignore the brighter surface and occlusion cues of the central illusory area in the Kanizsa illusion and focus only on the contour creation. Because the filling-in and the relative depth can be simulated if my *Physarum* model is coupled with a particular mechanism, the significance of my model and the real *Physarum* should not be lost.

In this study, I demonstrate that my model for foraging *Physarum* can reveal Kanizsa illusory contours if the pac-man faces the center, whereas the illusory contours disappear if the pac-man faces outward. In this result regarding stimulation, the pac-man is implemented as an attractant in the automata-fashioned model. I also demonstrate that the same patterns are obtained in the experiment involving the real plasmodium of the *Physarum*. In this case, the pac-man is implemented using a nutrient-rich dry agar sheet. These observations suggest that the transfer of biological information resulting from the synthesis of local and global interactions can create what is called extended visual perception, thus allowing visual illusion, i.e., biological and/or unconventional computing can emulate the perception of humans.

2.2 Material & Method

2.2.1 Definition of the model

Models of *Physarum* plasmodium have been suggested. For example, weighted graph model [31, 32], particles model [14] and network growth model ([29]), and so on. I use the Vacant-Particle (VP) model proposed by Gunji et al. [9, 10] to explain the adaptive network of the plasmodium of *Physarum*. This is an asynchronous cellular automaton defined on a discrete lattice plane in which the asynchronous application of transition rules provides amoeboid motility. This model has the advantage of not only simulating the amoeboid cellular motion of *Physarum* but also forming adaptive networks that depend on the surrounding environment [21, 11, 30].

First, I explain the basic algorithm of the model. The additional rules coupled with the model are defined later. The coordinates of a site on the discrete lattice plane are described by a pair of integers (i, j). For all sites (i, j), a binary value $c(i, j)$ is assigned. $c(i, j) = 1$ indicates that the site (i, j) is filled with the plasmodium and implies that the site is inside of the plasmodium. These are called internal sites. Similarly, $c(i, j) = 0$ indicates that the site (i, j) is outside the plasmodium. These are called external sites. In particular, an internal site that confronts at least one external site in a von Neumann neighborhood is defined as a membrane. In the left column of Fig.2.3 the normal internal sites are yellow, and the membrane sites are orange, whereas the external sites are not colored.

I use the symbol N to indicate an aggregation of internal sites.

$$N = \{(i, j) \mid c(i, j) = 1\} \tag{2.1}$$

14

Similarly, the symbol M indicates an aggregation of membrane sites.

$$M = \{(i,j) \in N \mid c(i+1,j) = 0 \lor c(i-1,j) = 0 \lor c(i,j+1) = 0 \lor c(i,j-1) = 0\} \tag{2.2}$$

Next, I explain the processes that provide amoeboid cell motility for N. Note that the word "neighborhood" means "von Neumann neighborhood".

The temporal transition of a plasmodium from time t to time $t+1$ is illustrated in the left column of Fig. 2.3. There are four child processes in the background of this change, and these are depicted in the right part of Fig. 2.3 (i)-(iv).

(i) I randomly choose one site from M. This selected site is called the stimulus point (SP). The SP is colored blue in Fig. 2.3(i).

(ii) Because the SP is a membrane cell, there is at least one external site in the neighborhood of the SP. I also randomly select an external site from among these neighbors. This selected external site is called the growth point (GP). The protoplasm at SP then moves to GP. This movement means that the value c at the GP changes to 1. Instead of this movement, an external void inserts into the SP. The void that has entered the plasmodium is called the vacant particle (VP).

(iii) The VP migrates between the internal sites N by exchanging places with neighboring internal sites. This sequential movement of the VP mimics a protoplasmic flow. The most important condition is that the protoplasm experiencing an exchange itself produces a gel transition. Because of this, these cells are never exchanged with the VP again. Therefore, the migration pathway of the VP never intersects with itself. The red-colored sites in
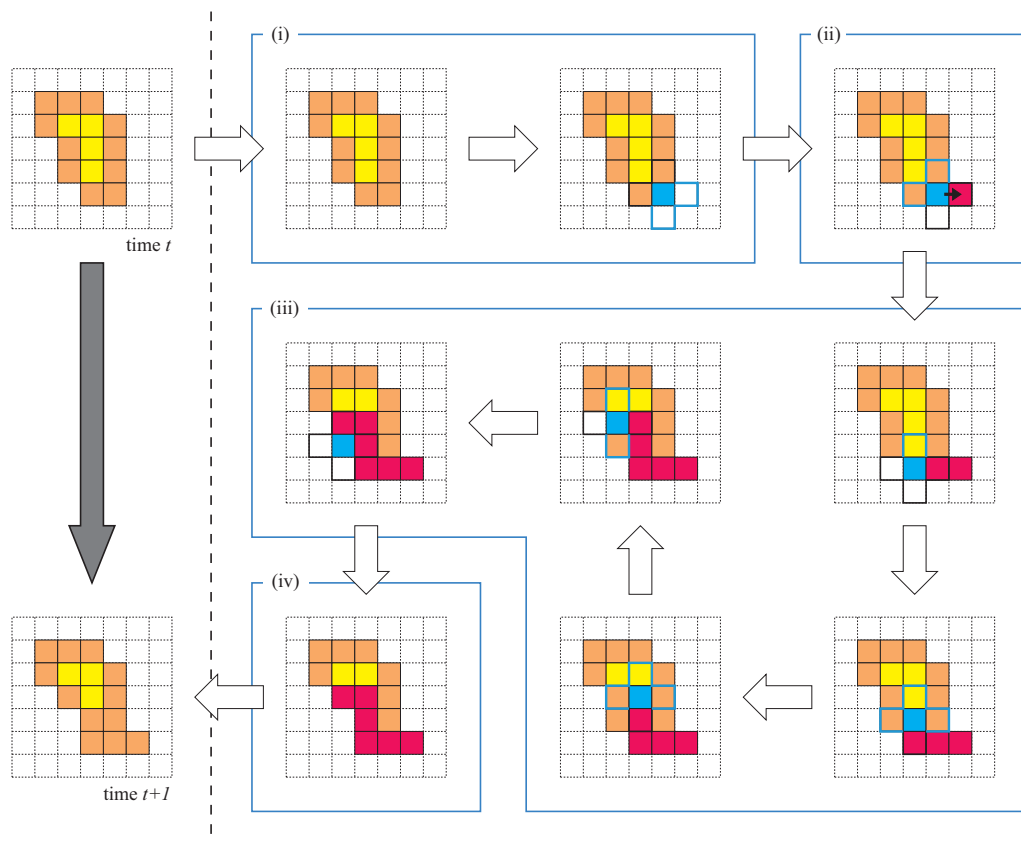
15

Figure 2.3: Basic algorithm of the model. The left column indicates the time evolution of the model from time t to $t + 1$. The right-hand portion indicates the four child processes: (i) the choice of stimulus point; (ii) the growth to the outside and entry into the VP; (iii) the migration of VP with a gel transition; and (iv) the escape of VP.

16

Fig. 2.3(iii) indicate the gelled protoplasm. The VP continues searching exchangeable cells in the neighborhood and exchanging places if possible.

(iv) In the case where the VP has no exchangeable neighborhood sites or the VP has exchanged a particular given number of times, the VP escapes from the plasmodium. This site is called the escape point (EP). Then, the value c at the EP becomes 0. Eventually, we observe that the protoplasm that was at the EP has moved to the GP. Therefore, these processes conserve the number of internal sites. i.e., the covered area by plasmodium does not change temporally. Finally, the entire gelled protoplasm undergoes a sol transition.

This is the basic algorithm of the model. These processes are called the "one time step", i.e., they occur all at once. The characteristic of this model is a gel transition. This condition maintains the integrity of the plasmodium and enables amoeboid motion. However, this basic model *Physarum* cannot move over a long distance because the random selection of the SPs and GPs prohibits unidirectional growth. Hence, to acquire real *Physarum* plasmodium-like behavior, some taxis must be defined regarding this model. In fact, the introduction of the localization of probabilities to the random choice process yields taxis for the model.

2.2.2 Additional rules

It is well known that real *Physarum* plasmodium has a negative taxis to white light. Thus, I propose an Avoid Bright region VP (ABVP) model as defined below.

For all sites (i, j) on the lattice plane, a new binary value $b(i, j)$ is defined. This value $b(i, j)$ corresponds to the brightness of the site. $b(i, j) = 1$

indicates that the site is bright, and $b(i, j) = 0$ indicates that the site is dark.

   In the basic model, there are three types of random choice processes, which are detailed below.

  1. The choice of the SP.

  2. The choice of the GP.

  3. The choice of the direction of movement of the VP .

For each of these processes, we introduce variations of probabilities.

The choice of the SP.

First, for all sites (i, j), I define the integer value $s(i, j)$ depending on $c(i, j)$ and $b(i, j)$. The value $s(i, j)$ is determined as follows [Fig. 2.4(i)]:

$$s(i, j) = \begin{cases} 0 & (c(i, j) = 1) \\ 1 & (c(i, j) = 0 \land b(i, j) = 1) \\ 2 & (c(i, j) = 0 \land b(i, j) = 0). \end{cases} \quad (2.3)$$

Next, the new value $w(i, j)$ is defined for all of the membrane sites depending on $s(i, j)$, as defined in the equation below.

$$w(i, j) = s(i + 1, j) + s(i - 1, j) + s(i, j + 1) + s(i, j - 1). \quad (2.4)$$

Here, $w(i, j)$ reflects the local environment of the site (i, j). This $w(i, j)$ value determines the probability $p_s(i, j)$ that the membrane site (i, j) will be selected as the SP.

$$p_s(i, j) = \frac{w(i, j)}{\displaystyle\sum_{(m,n) \in M} w(m, n)}. \quad (2.5)$$

Therefore, the membrane sites that have many external and dark neighborhoods are selected with a high probability.

18

The choice of the GP.

Let a membrane site (i, j) be selected as the SP. The GP is then determined using the probabilities described below.

For a neighbor site of the SP (i, j), which for convenience I write as (i', j'), the probability $p_g(i', j')$ that the site (i', j') will be selected as the GP is determined by the value s that was previously defined in [Fig. 2.4(ii)].

$$p_g(i', j') = \frac{s(i', j')}{s(i+1, j) + s(i-1, j) + s(i, j+1) + s(i, j-1)}. \tag{2.6}$$

Note that if a neighboring site is internal, then the probability choice becomes 0 because of the definition of s.

The choice of the direction of movement of the VP.

The above two conditions promote biased growth toward the dark sites. Next, I introduce another rule to implement repellency from the bright region. To decrease the plasmodium under the bright area, the VP is expected to move toward the brighter area. Let the VP be at the site (i, j); then for all neighbor sites (i', j') of the VP, a value $r(i', j')$ is defined as follows [Fig. 2.4(iii)]:

$$r(i', j') = \begin{cases} 0 & (c(i', j') = 0 \vee (i', j') \text{ is gelled}) \\ 1 & (c(i', j') = 1 \wedge (i', j') \text{ is not gelled} \wedge b(i', j') = 0). \\ 2 & (c(i', j') = 1 \wedge (i', j') \text{ is not gelled} \wedge b(i', j') = 1). \end{cases} \tag{2.7}$$

The probability $p_m(i', j')$ that the neighbor site (i', j') will be chosen as the next destination of the VP is then determined as in the following equation:

$$p_m(i', j') = \frac{r(i', j')}{r(i+1, j) + r(i-1, j) + r(i, j+1) + r(i, j-1)}. \tag{2.8}$$
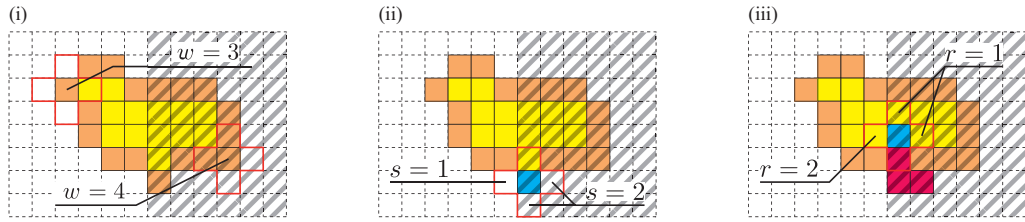
Figure 2.4: The right part of each figure is dark, and the other area is bright. (i) The membrane at the dark site is chosen more frequently. (ii) Growth is attracted to the dark site. (iii) Avoidance of the bright area.
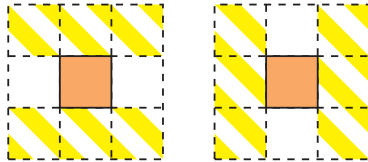

Figure 2.5: Examples of linear structure. The central sites are linear structure. It does not matter whether the shaded area are the protoplasm or not.

Linear structure correction.

An internal site (i, j) is called a "linear structure" if both sides of (i, j), $(i+1, j), (i-1, j)$ or $(i, j+1), (i, j-1)$ are external sites(Fig.2.5).

During the process of randomly choosing a stimulus point, if a candidate site (i, j) is a linear structure, then a positive constant L is added to $w(i, j)$. From previous work ([11]), it is known that a larger value of L produces a straighter linear network. However, a value for L that is too large will invalidate the negative taxis for the bright regions. Therefore, in this paper, the value of L was set to 10.

Thickness rules.

In the basic algorithm, the number of internal sites does not change throughout the development. This implies that the area covered by the model plasmodium is unchanged. A real *Physarum* plasmodium, however changes its cell thickness spatiotemporally to spread widely or concentrate in a narrow area. In particular, under the condition that I consider here, a real plasmodium would likely converge upon dark regions, and its cell thickness would increase.

To implement this behavior, I add the next two rules to my model. Let (i_g, j_g) be the GP and (i_e, j_e) be the EP at the time step t.

After the escape process,

1. if $b(i_g, j_g) = 0$ and $b(i_e, j_e) = 1$, then $c(i_g, j_g) = 0$,

2. if $b(i_g, j_g) = 1$ and $b(i_e, j_e) = 0$, then $c(i_e, j_e) = 1$.

What do these rules mean? 1. If the protoplasmic flow moves from a bright region to a dark region, then protoplasm is used to increase the thickness at the stimulus point. Accordingly, the growth process appears to be halted

(Fig. 2.6(i)). 2. In contrast, if the protoplasm moves from a dark region to a bright region, then the cell thickness at the dark region decreases instead of protoplasmic spreading at the bright region. This rule invalidates the escape process [Fig. 2.6(ii)].

The former rule decreases the area covered by the plasmodium, and the latter rule increases this area. These rules are applied deterministically depending on only the brightness at the GP and the EP.

Fluctuation.

The final additional rule is related to fluctuations. At each time step, the definition of the value s, which was given in section 2.2.2, is changed with the probability p_f such that

$$s(i, j) = \begin{cases} 0 & (c(i, j) = 1) \\ 1 & (c(i, j) = 0) \end{cases} \text{(with } p_f\text{)}. \tag{2.9}$$

The linear structure correction is not applied here. Therefore, the stimulus point is chosen depending on only the local information regarding the state of the sites. Because the SP is chosen uniformly, this rule accordingly promotes growth in the bright region, which results in the reconstruction of the networks. As a result, shorter networks are given. In this paper, I set $p_f = .05$.

2.2.3 Experimental configuration

The model

A detailed description of my *Physarum* model is provided herein. Pac-men in the Kanizsa diagram are defined as dark regions, and other areas are defined as bright regions [Fig. 2.7(a)]. For the control experiment, the pac-men in
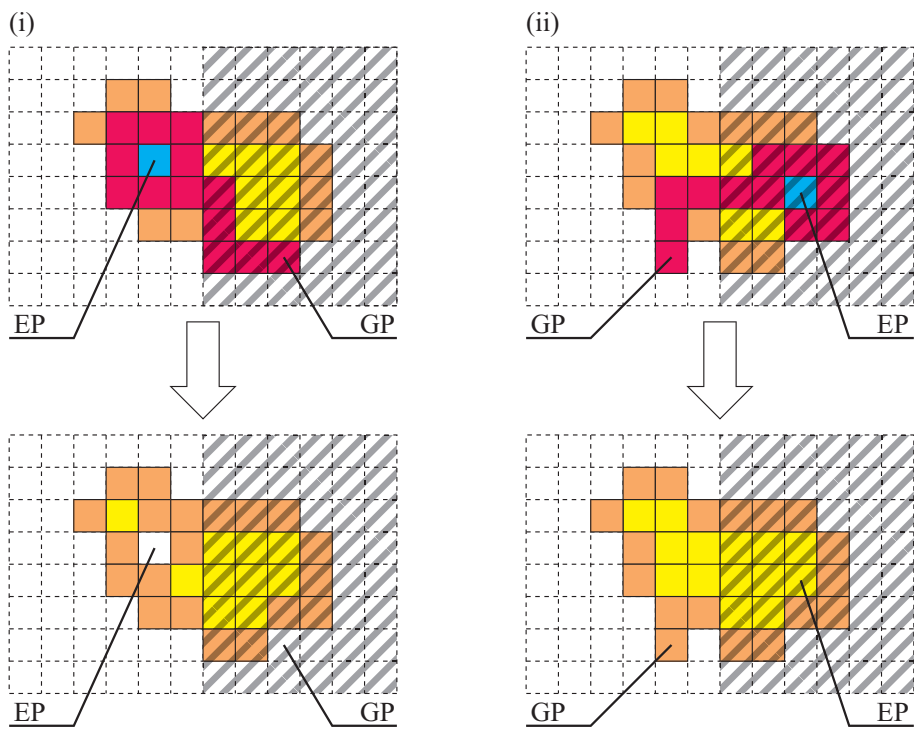
Figure 2.6: Thickness rules. (i) If GP is dark and EP is bright, then $c(\text{GP}) = 0$, and the covered area decreases. Conversely, (ii) if GP is bright and EP is dark, then $c(\text{EP}) = 1$, and the covered area increases.

the Kanizsa diagram are turned 180 degrees [Fig. 2.7(b)]. Clearly, in the case of the control, the illusory contour does not appear in the perception of humans. The resolution of both of these images is 120×120 pixels. The lattice plane on which the models are defined has the same size.

I conducted experiments 100 times for each image and examined the network topology obtained after 5 million time steps for each experiment. The maximum limit for the number of VP movements for each time step was set at 300. The initial state of the plasmodium was determined using the following method:

1. For all sites on the lattice plane, I defined $c = 1$;

2. A site that has a value $c = 1$ was randomly chosen as the SP;

3. The VP enters the plasmodium at SP, although growth does not occur;

4. The VP migrates between the internal sites conforming to the rules of the VP model and eventually stops;

5. The site at which the VP stops becomes $c = 0$ (Because the growth process was halted, the area covered by the plasmodium decreases by one site);

6. Repeat 2-5 until the entire covered area is reduced to $< 45\%$ of the area of the entire lattice plane.

This method provides cancellate networks that cover the entire plane with many medium-size holes. These networks imitate the real *Physarum* tubular networks that are formed on an unstimulated agar plate.

In addition to simulation studies, I conducted a real plasmodium experiment in which pac-men in the Kanizsa diagram are implemented with nutri-

ent rich agar (attractant). In the next section, I describe the experimental configuration for a real plasmodia experiment.

Real plasmodia

I cultivated *Physarum* plasmodia using the method of [4]. Briefly, the plasmodia were cultured on wet paper towels laid out on glass Petri dishes in a plastic box. The space below the towels was filled with tap water to maintain humidity. Oatmeal flakes were provided daily as food. I maintained the culture environment in the dark at 25 °C.

In this study, I introduced a sheeted food source made from nutrient-rich agar to make attractant figures. The sheet was easily shaped into various figures and sizes. The nutrient-rich sheet was produced as follows: 400 ml of a solution containing 1.5% agar and 20 mg/ml oatmeal powder was poured into a 295×220 mm plastic tub; the resulting sheet was dried thoroughly in a natural convection oven at 50 °C.

In the experiment, I made three pac-men from the above nutrient agar sheet. The radius of a pac-man was 5 mm, and the distance between the centers of two pac-men was 15 mm (Fig. 2.8). I used a 1.5% unamended agar plate in a 9 cm diameter Petri dish as an experimental field. I put the agar sheet pac-men onto the plain agar plate in a fixed arrangement and kept it at rest until the sheets were rehydrated (approximately one hour). Next, I inoculated 5 mg of plasmodial fragments onto the center of each of pac-man and photographed the plasmodia at intervals of 30 minutes. I captured images using a single-lens digital camera (EOS Kiss X6, Canon, Japan) from directly above, and the experimental system was kept at 25 °C. I repeated the experiments 24 times and performed the same number of control experiments.
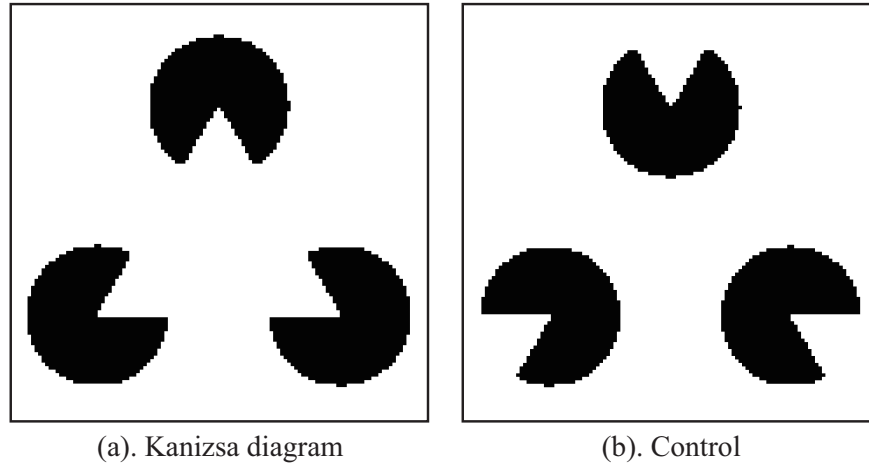
(a). Kanizsa diagram   (b). Control

Figure 2.7: Stimulus figures are given as geometrical patterns of brightness (black or white). (a) Kanizsa diagram and (b) control figure.
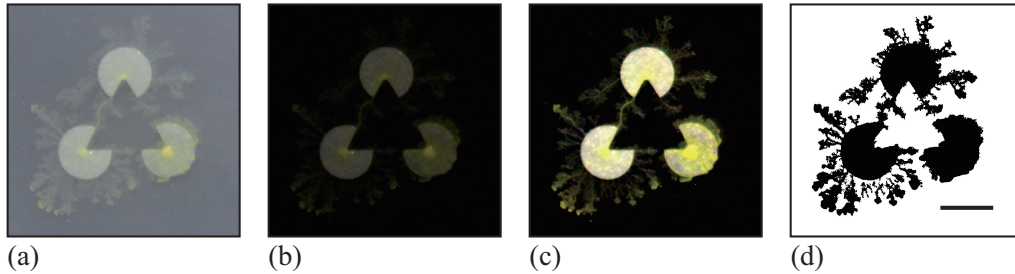

(a)   (b)   (c)   (d)

Figure 2.8: Experiment using real *Physarum* (scale bar: 10 mm). The radius of a pac-man was 5 mm, and the distance between the centers of two pac-men was 15 mm. (a) The captured image. (b) Obtained by subtracting the background of (a). (c) Adjusted the brightness. (d) binarization. All processes were executed by using the ImageJ software. In the binary image, the plasmodia are indicated by black pixels. The threshold of binarization is determined not to delete delicate structure of plasmodium.

2.3 Results

2.3.1 Model results

I classified the resulting networks based on their topology. The networks were divided into four types [27] (Fig. 2.9) as follows:

- type I is a triangle that connects three pac-men;

- type II is a V-shape obtained from a triangle lacking of side;

- type III has another node that links with all of the pac-men and one side of a triangle;

- type IV is a simple star structure.

However, for the Kanizsa diagram, there were a few undifferentiated networks that could not be classified any of the above types. Therefore, all of networks these were categorized together as "others" and excluded from the following statistical test. Obviously, type I networks complement the illusory contour of a Kanizsa diagram.

The frequencies of each type are given in Table 1. Clearly, in the case of the Kanizsa diagram, type I networks were obtained more frequently than the control case. Type IV networks were not obtained at all, while this type comprised over 40% of the resulting networks in the control case. A χ-square test indicated that there was a significant difference between these two data [χ-square$(3, N = 191) = 56.7$, $p < .001$]. Therefore, this difference in the frequencies between the Kanizsa triangle and the control figure reflects the difference in the configuration of the pac-men.

What was the cause of this difference? To clarify this, I illustrate an example of the time development of the network for each stimulus image
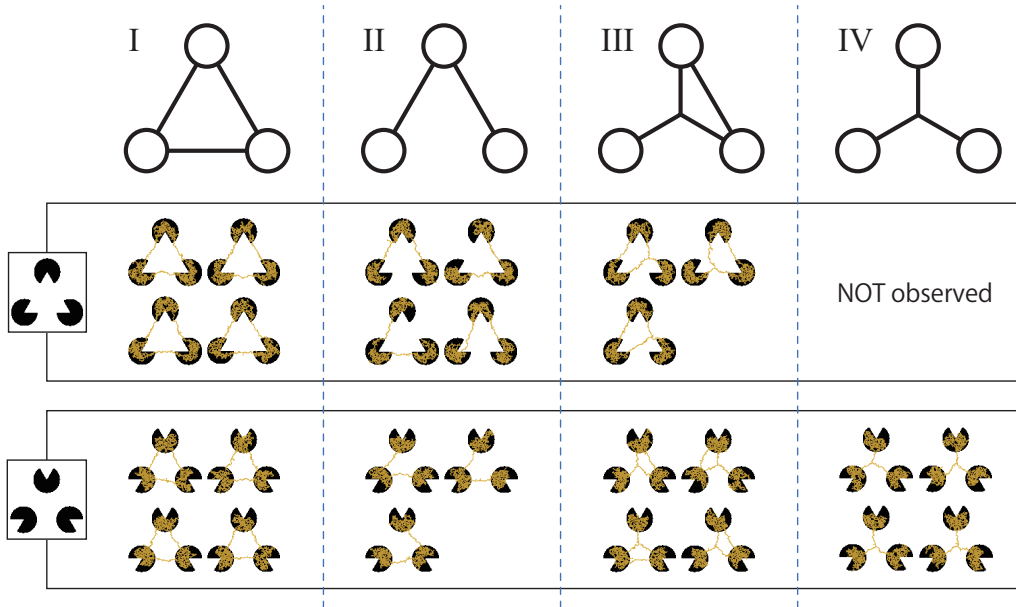
Figure 2.9: Classification of the resulting networks according to their topology. Type I is a triangle; type II is a V-shape; type III is a slingshot-like shape; and type IV is a star or Y-shape. A type IV network was not obtained for the Kanizsa diagram.

Table 2.1: The frequency of network types for two stimulus patterns.

Stimulus image	type I	type II	type III	type IV	others	total
Kanizsa diagram	79	9	3	0	9	100
control	46	3	8	43	0	100

(Fig. 2.10). In the case of the Kanizsa diagram, the illusory contour is very stable. It formed completely before $t = 2,000,000$ and was maintained until $t = 5,000,000$. In contrast, in the control, the network changed over time and was not stable. This is a general disposition of the types in Table 1. According to this perspective, the explanation of the difference is a difference in the stability of the *Physarum* network for each stimulus image. This suggests the presence of a unique potential structure for each image. The lack of a mouth for the pac-man may work as some sort of "energy barrier" for the plasmodial networks. In the Kanizsa diagram, these barriers produced the triangular networks because all of the pac-men were arranged face-to-face. However, the configuration of the control figure did not work similarly. In this sense, the resulting networks reflected the global configuration of the pac-men.

2.3.2   Results using real plasmodia

In these experiments, I compared real *Physarum* networks with my model. Because the real plasmodia networks usually have more complex structures than my model (Fig.2.11), the classification of network types is not obvious, unlike the model cases. Therefore, I adopted another analytical method to estimate the spatial distribution of the plasmodia.

The captured images of the real plasmodia were processed using ImageJ image processing software [23]. Fig.2.8 shows each step of the binarization process for the image. Fig.2.8 (a) is the original photograph, and (b) is obtained using "Subtract Background", a macro function of ImageJ, on (a). The "Adjust/ Brightness and Contrast" command to automatically normalize the brightness produces image (c). The threshold of binarization is determined according to the brightness value of the site on which the
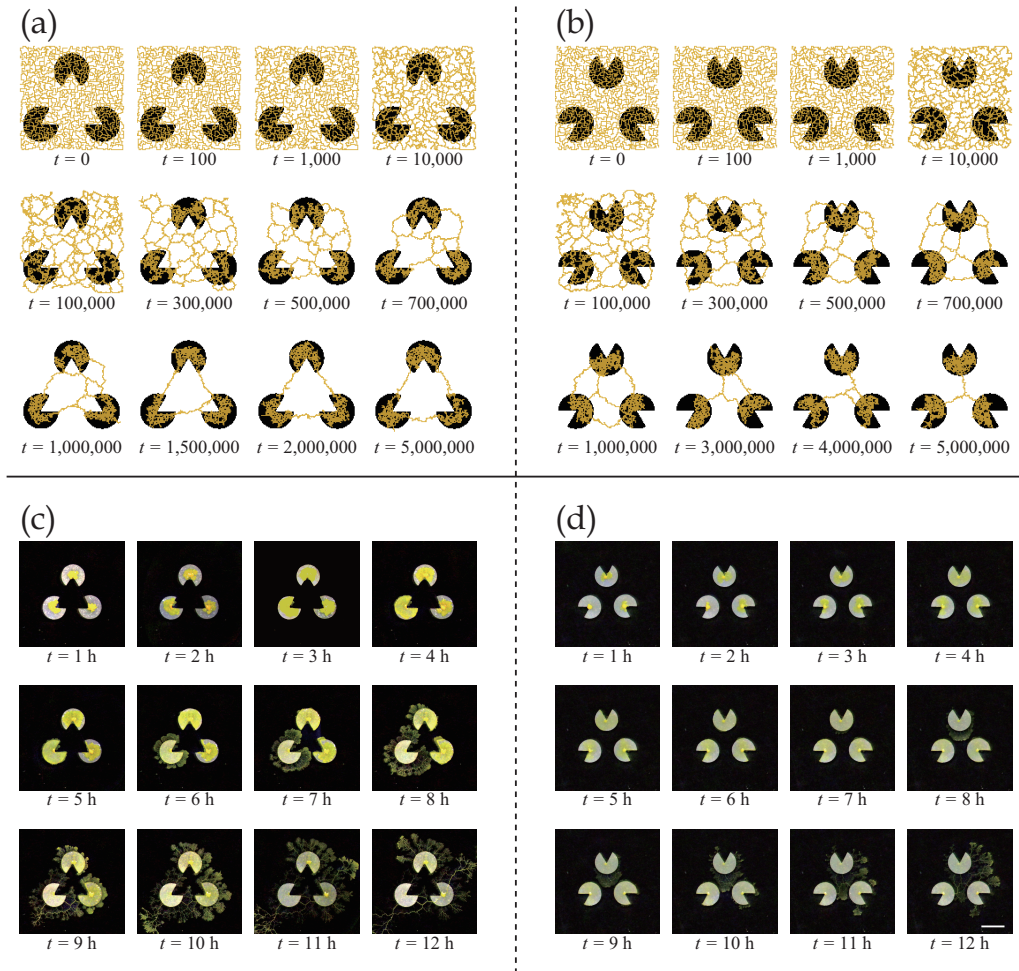
29

Figure 2.10: Typical evolution of the networks of model (a, b) and real plasmodium (c, d) (scale bar: 10 mm). (a) For the Kanizsa diagram, the network structures are highly stable. (b) In the control diagram, the network changes gradually and becomes shorter. (c) The plasmodium does not enter the central area of the illusory triangle. (d) The plasmodia occupy the middle area of the pac-men.
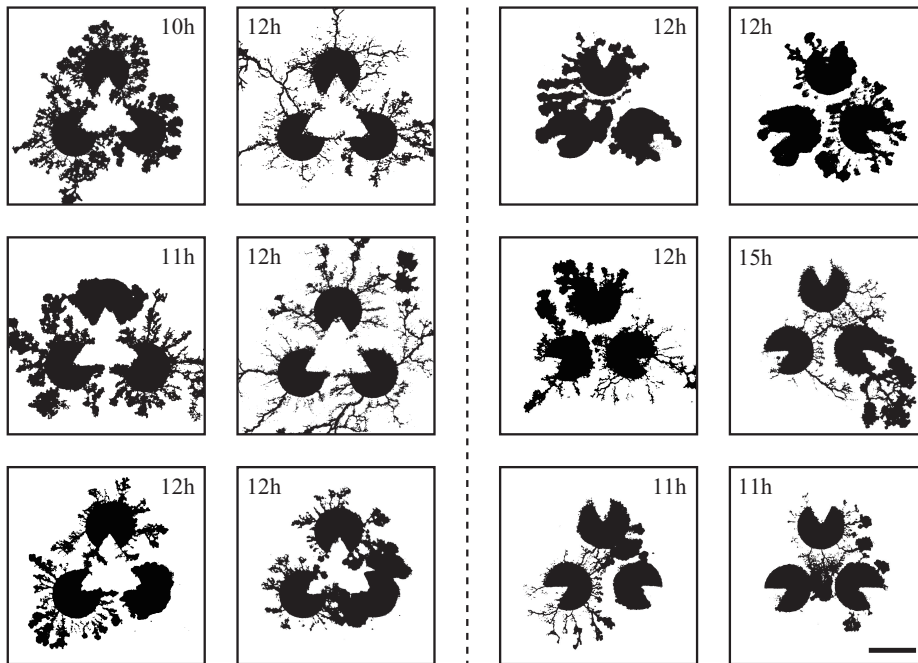
Figure 2.11: The resulting networks from the real *Physarum* experiment (scale bar: 10 mm) corresponding to the Kanizsa diagram (a) and the control (b). The time stamp of each networks are shown in the image. Note that these networks are the results of individual trials and these photos are not in a time series.

plasmodia are thinly spread to maintain the delicate structures. Obvious noise surrounding the plasmodium, such as dust or bubbles in the agar plate are removed manually. Finally, the binarized image (d) is obtained. The time series of plasmodial networks are shown in Fig.2.10 (c, d), and some examples of the binarized images of the networks are shown in Fig.2.11. According to these images, the plasmodium rarely entered the central area of the illusory triangle in the case of the Kanizsa diagram. In contrast, the corresponding areas of the control figures are occupied by the plasmodium.

To clarify this, I produce Fig.2.12 by stacking binarized images for all of the trials. Because the initial configuration has rotational symmetry, the images that are 120° and 240° rotations of the original are also used. In Fig.2.12, the brightness of each site indicates the intensity of lapping, which is the probability of the plasmodium being at the site. The sites that are occupied more frequently have higher brightness levels. Therefore, the whole image represents the distribution of the probabilities. I have used the "Lookup table/Yellow Hot" color chart in ImageJ. To improve the visibility of the figures, a filter was applied to cut off the weak signals. This threshold is determined as 10% of the theoretical maximum of the signal, and this value is common to both conditions. To remove the effects of Kanizsa illusory contour, the pac-men are covered with black in the lower row. Obviously, the type I-like structure is apparent in the Kanizsa diagram case, and the structure that is the sum of type I and type IV networks appears in the control. This observation does not conflict with my model results because type I networks appeared dominantly in the Kanizsa diagram case, but in the control, type I and type IV networks were obtained in almost the same ratio. Next, I emphasize this difference numerically.

I defined the target region of evaluation as depicted in Fig.2.13. The

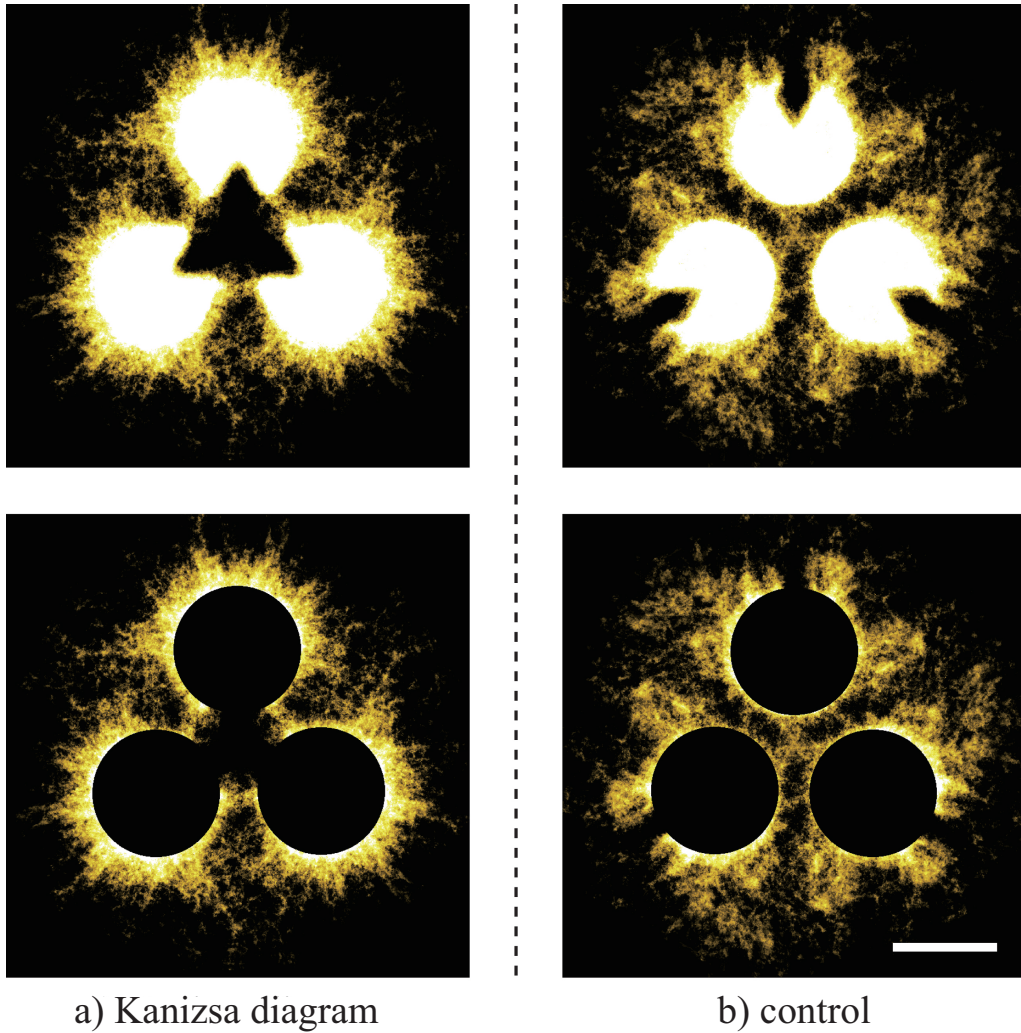a) Kanizsa diagram   b) control

Figure 2.12: The upper diagrams are produced by stacking binaralized images of the plasmodial networks for all trials. The brightness of each site indicates the intensity of lapping; that is the existence probability of the plasmodium at the site. A filter that cuts-off the weak signals was applied to improve visibility. This threshold is common to both figures. In the lower diagrams, to wipe out the effect of Kanizsa illusory contour, the pac-men are covered by black (scale bar: 10 mm).

yellow-colored marginal area of the fan that centers a pac-man was divided into six regions. All of these fans had the same central angle of 15° and were labeled A to F according to the direction from the center. The same labeled areas were identified. For each region, the ratio of the area occupied by plasmodium was measured. I precisely counted the number of black pixels, which indicated that the site was occupied by plasmodia in the binary converted images (see, for example, Fig.2.8 (d)). To normalize the values, the number of black pixels was divided by the total number of pixels for each region. The relationships between the mean values of the occupation ratios and directions are plotted in Fig.2.14.

In the Kanizsa diagram cases, the plasmodia converged to areas A and F. In contrast, in the control cases, the *Physarum* spread uniformly, and there was no clear peak. In the model case, there were significant differences in the occupation ratios between the two figures for all areas at a 0.1% level according to the Wilcoxon rank sum test (A: $W = 74,996$, $p < .001$; B: $W = 34,774$, $p < .001$; C: $W = 26,542$, $p < .001$; D: $W = 26,952$, $p < .001$; E : $W = 37,559$, $p < .001$; F: $W = 74,480$, $p < .001$). Similarly, in the case of actual plasmodia, I could see that there were significant differences at the same level for only areas C and D, which occupied the center of fan (A: $W = 2,795.5$, $p = .416$; B : $W = 2,402$, $p = .448$; C: $W = 937$, $p < .001$; D: $W = 1,085$, $p < .001$; E : $W = 2,335$, $p = .304$; F: $W = 2,753$, $p = .52$). In this regard, the results of the model and the real plasmodia are highly consistent. Namely, the illusory contour of the Kanizsa diagram is complemented by the plasmodia in both cases. These results are derived from the directed cell motility depending on the configuration of the attractant.
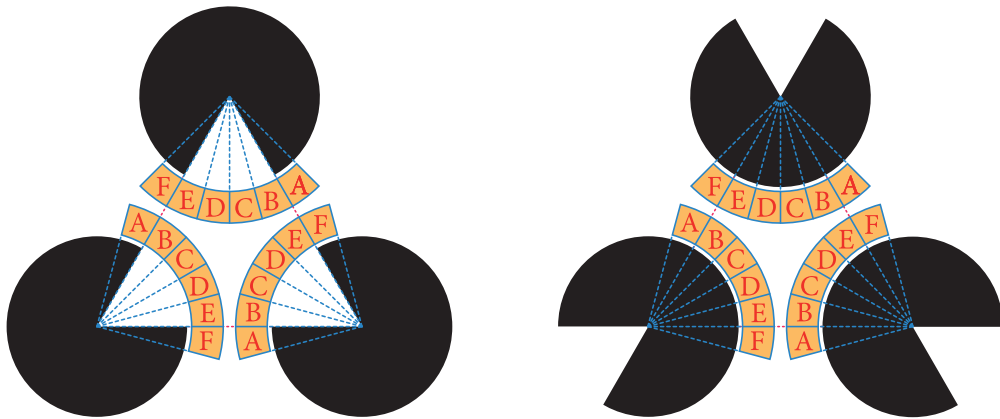
Figure 2.13: Target region of analysis. The marginal areas of the fans that are colored yellow are divided into six regions and named A - F according to the direction. For each divided region, I counted the number of black pixels and estimated the area covered by the plasmodium. An occupation ratio of a region is given as the ratio of covered area to the total area of the region.
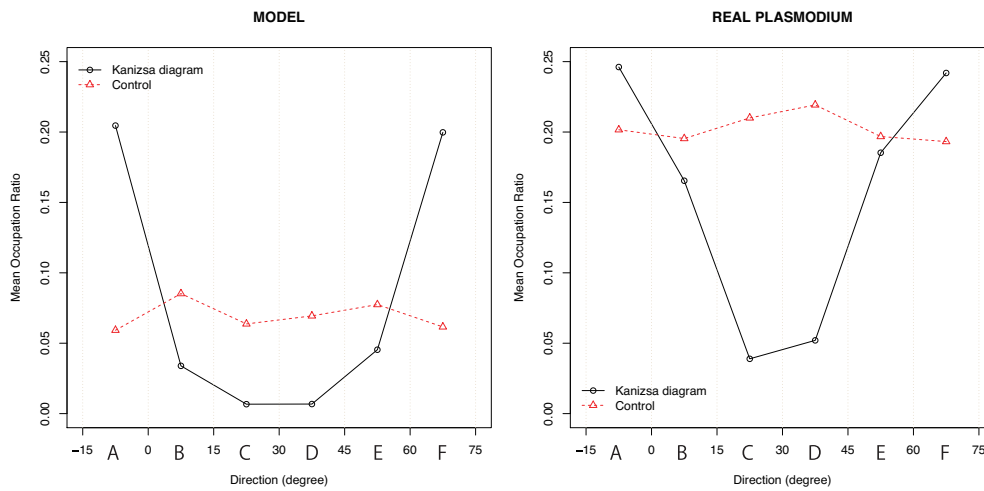
Figure 2.14: The relationship between the mean value of the occupation ratio and direction. For the Kanizsa diagram, there are two peaks at region A and F in both experiments. In the model case, type I and type III networks canceled each other out. Therefore, a clear peak does not appear. There is also no peak in the real plasmodium case because of the isotropic growth of the plasmodium.

2.4 Discussion

These results demonstrate that our visual perception of the illusory contours of the Kanizsa diagram can be emulated by both the asynchronous automata-fashioned model and by real plasmodia as an analogy at the phenomenological level. This finding does not mean that the plasmodia have human-like intelligence or perceptive faculties. It is clear that *Physarum* plasmodia cannot be a direct model of our brain because plasmodia do not have even primitive nervous systems. Nevertheless, I can say that there is abstract homogeneity between plasmodial behavior and nervous activity in our brain. This analogy has meaning at a mechanistic level.

It is known that our consciousness contains perception and feeling arising from neural information that is processed in our brains. The causality between particular activities of neurons and our consciousness has not been sufficiently investigated. Nevertheless, I can regard this nervous activity as a type of "computation" that is calculated by complex neuronal firing patterns. In other words, I can say that our consciousness is a product of a program consisting of multiple neural networks. Obviously, I cannot consider that the program is the same as an ordinary computer program at the syntactical level. However, the semantics of the program can be discussed. Taking this perspective, it is possible that the perception arising from brain activity is analogous to plasmodial behavior, which is of a different material and complexity altogether.

To perceive the illusory contours of the Kanizsa diagram, both the differentiation and integration processes are necessary. Depending on the local gradient of the stimuli, detection of the edge of the pac-man corresponds to a differential process, and the combination of the local data based on their global configuration corresponds to an integral one. Therefore, the former is

a lower-order process that finds the difference in stimuli in a relatively narrow area on the retina, and the latter is a higher-order process that integrates this information and constructs a visual field. This means that the illusory contours appear with a sort of information contraction from lower to higher orders.

What plasmodial behavior corresponds to the each of differential and integral processes? Plasmodia search their surrounding environment and react to the attractant and the repellant. This is differential. For integration, plasmodia propagate local information using protoplasmic flow to decide their overall behavior. In our model, the imbalance of the choice of SP depending on the local state and the movement of VP based on asynchronous application of the transition rules corresponds to the differential and integral processes respectively. Therefore, the model and real plasmodia have analogous functionality to the processes of visual perception of the illusory contours. In this way, plasmodia can combine lower and higher-order information smoothly without a specialized pivotal organ, such as a nerve center, that oversees the entire system.

It is important to note that the resulting networks' complementary illusory contour cannot be obtained as an optimized network at the global level. Actually, We can link all of the pac-men with more shorter paths. For example, the V-shaped network (type II) and the Steiner tree (star shape, type IV) have more total shorter paths than the triangular network (type I). However, these networks were not generally obtained in either experiment. If the plasmodia oversee the whole and choose optimized networks, triangular networks would not appear. This means that the illusory contours seem to result from the redundancy of the network, which is considered to be an error or mistake in the *Physarum* computer studies that consider some

optimization problems.

In the Kanizsa diagram, the mouth of a pac-man works as an obstacle to change shorter paths and provides metastable networks such as in type I because all pac-men are face-to-face. However, in the control, all pac-men are back-to-back, and the mouths of the pac-men do not behave as barriers. Then, the transition of the network structure to a more stable and shorter network occurs quickly. This indicates that the resulting networks reflect the potential structure of each spatial configuration of pac-men.

The use of an analogy to recognize that plasmodial behavior and visual perception have the same functionality provides us with one perspective about the origin of illusory contours. When we pick out information from our visual field, it is important to determine the borders of the objects using gradients of stimuli such as brightness or color. However, it is inefficient to process all local information at the same level because the volume of information is too huge. Therefore, to efficiently find the border, we must compress the local information to some extent. In this way, I can say that illusory contours are a by-product of the information contraction corresponding to the moderate optimization of the plasmodial networks in my analogy.

I have equated the plasmodial behavior and our perception at the mechanistic level and discussed the analogous homogeneity between them. Finally, I refer to a point of difference between my study and previous studies concerning *Physarum* computation. Whereas I used the true slime mould plasmodium as a computational device for a visual perception model, in conventional works, plasmodia have been used for optimization problems. I can say that the latter viewpoint considers *Physarum* computation to be an effective bio-inspired algorithm, similar to a genetic algorithm or a neural network.

My perspective is completely different. I am attempting to understand the computational processes of organisms through a model based on bio-computation. A bio-computer is the most suitable device for modeling the computational processes of an organism. To understand biological computational processes, it is necessary and important to construct models of these processes using a bio-computer and to discover the abstract connections between the model and the phenomena. My experiments are a starting point for *Physarum* computational studies that suggest the computability of our "perception" and "feeling".

Chapter 3

Conclusion

I showed that both the model and real *Physarum* plasmodia can reproduce Kanizsa illusory contour. The interaction between each computation at "Mono" and "Koto" levels permits this complementation. Thus, the plasmodia have fundamental functionality that models our sensitivity in abstract level. This results provide a new perspective about origin of sensitivity and qualia.

The problem of qualia is usually discussed in a context of the gap between neural activity ("Mono") and consciousness ("Koto"). A characteristics of this question are equal to the question "What is the heap?", and we cannot answer this type of question in "Mono" level. Therefore, It is an ill-posed problem.

I consider our sensitivity including qualia is the result of interaction between differential "perception" and integral "feeling". And in *Physarum* plasmodia, this interaction is executed as the reaction to the stimuli and the integration of such local information. These two processes are connected by protoplasmic flow that is seems to invalidate the gap between "Mono" and "Koto". To understand the emergence, it is necessary to introduce a particular mechanism invalidate the difference between "Mono" and "Koto".

In this viewpoint, the problem of qualia can be discussed as the level of functionality of computation. And then, the problem will become well-posed one. It is a turning of attitude toward our sensitivities and this is maybe a only valid approach to this phenomena.

Acknowlegement

Bibliography

[1] A. Adamatzky. *Physarum* machines: encapsulating reaction–diffusion to compute spanning tree. *Naturwissenschaften*, 94:975–980, 2007.

[2] A. Adamatzky. *Physarum Machines: Computerrs from Slime Mould.* World Scientific, Singapore, 2010.

[3] A. Adamatzky, R. Armstrong, J. Jones, and Y. P. Gunji. On creativity of slime mould. *International Journal of General Systems*, 2013.

[4] W. G. Camp. A method of cultivating myxomycete plasmodia. *Bull. Torrey Bot. Club*, 63:205–210, 1936.

[5] S. Coren. Subjective contours and apparent depth. *Psychological Review*, 79:359–367, 1972.

[6] B. Gillam and K. Nakayama. Subjective contours at line terminations depend on scene layout analysis, not image processing. *Journal of Experimental Psychology: Human Perception and Performance*, 28:43–53, 2002.

[7] S. Grossberg. 3-d vision and figure ground separation by visual cortex. *Perception & Psychophysics*, 55:48–120, 1994.

[8] S. Grossberg and L. Pessoa. Texture segregation, surface representation and figure– ground separation. *Vision Research*, 38:2657–2684, 1998.

[9] Y. P. Gunji, T. Shirakawa, T. Niizato, and T. Haruna. Minimal model of a cell connecting amoebic motion and adaptive transport networks. *J. Theor. Biol.*, 253:659–667, 2008.

[10] Y. P. Gunji, T. Shirakawa, T. Niizato, T. Haruna, and I. Balaz. Life driven by damaged damage. *Prog. Theore. Phys. Supp.*, 173:26–37, 2008.

[11] Y. P. Gunji, T. Shirakawa, T. Niizato, M. Yamachiyo, and I. Tani. An adaptive and robust biological network based on the vacant-particle transportation model. *J. Theor. Biol.*, 272:187–200, 2011.

[12] C. Q. Howe and D. Purves. The müller-lyer illusion explained by the statistics of image-source relationships. *PNAS*, 102:1234–1239, 2005.

[13] N. Humphrey. *Seeing red: a study in consciousness*. Harvard University Press, 2006.

[14] J. Jones. Characteristics of pattern formation and evolution in approximations of *Physarum* transport networks. *Artificial Life*, 16:127–153, 2010.

[15] G. Kanizsa. *Organization in Vision: Essays on Gestalt Perception*. Praeger Pub. Co., 1979.

[16] K. Koffka. *Principles of Gestalt psychology*. Harcourt, Brace & World, New York, 1935.

[17] N. Kogo, C. Strecha, L. V. Gool, and J. Wagemans. Surface construction by a 2-d differentiation–integration process: A neurocomputational model for perceived border ownership, depth, and lightness in kanizsa figures. *Psychological Review*, 117:406–439, 2010.

[18] F. C. Müller-Lyer. Zur lehre von den optischentaushungen über kontrast und konfluxion. *Zeitschrift für Psychologie und Physiologie der Sinnesorgane*, 9:1–16, 1896.

[19] T. Nakagaki. Smart behavior of true slime mold in a labyrinth. *Res. Microbiol.*, 152:767–770, 2001.

[20] T. Nakagaki, H. Yamada, and A. Toth. Maze-solving by an amoeboid organism. *Nature*, 407:470–470, 2000.

[21] T. Niizato, T. Shirakawa, and Y. P. Gunji. A model of network formation by *Physarum* plasmodium: Interplay between cell motility and morphogenesis. *Biosystems*, 100:108–112, 2010.

[22] L. Pessoa, E. Thompson, and A. Noë. Finding out about filling-in: A guide to perceptual completion for visual science and the philosophy of perception. *Behavioral and Brain Sciences*, 21:723–748, 1998.

[23] W.S. Rasband and ImageJ. U. S. National Institutes of Health, Bethesda, Maryland, USA, 1997-2013.

[24] W. D. Ross and L. Pessoa. Lightness from contrast: A selective integration model. *Perception & Psychophysics,*, 62:1160–1181, 2000.

[25] T. Sakiyama and Y. P. Gunji. The müller-lyer illusion in ant foraging. (in press), 2014.

[26] T. Shirakawa, A. Adamatzky, Y. P. Gunji, and Y. Miyake. On simultaneous construction of voronoi diagram and delaunay triangulation by *Physarum polycephalum. Int. J. Bifurcat. Chaos*, 19:3109–3117, 2009.

[27] T. Shirakawa and Y. P. Gunji. Emergence of morphological order in the network formation of *Physarum polycephalum*. *Biophys. Chem.*, 128:253–260, 2007.

[28] T. Shirakawa and Y. P. Gunji. Computation of voronoi diagram and collision-free path using the plasmodium of *Physarum polycephalum. Int. Journ. of Unconventional Computing*, 6:79–88, 2010.

[29] A. Takamatsu, E. Takaba, and G. Takizawa. Environment-dependent morphology in plasmodium of true slime mold *Physarum polycephalum* and a network growth model. *J. Theor. Biol.*, 256:29–44, 2009.

[30] I. Tani, K. Sonoda, J. Jones, and Y. P. Gunji. Emulation of ambiguous figure perceptions using the model *Physarum polycephalum*. In *Proceedings of the 2nd International Conference of Morphological Computation*, pages 94–96, 2011.

[31] A. Tero, R. Kobayashi, and T. Nakagaki. *Physarum* solver: a biologically inspired method of road-network navigation. *Physica A*, 363:115–119, 2006.

[32] A. Tero, R. Kobayashi, and T. Nakagaki. A mathematical model for adap- tive transport network in path finding by true slime mold. *J. Theor. Biol.*, 244:553–564, 2007.

[33] A. Tero, S. Takagi, T. Saigusa, K. Ito, D. P. Bebber, M. D. Fricker, K. Yumiki, R. Kobayashi, and T. Nakagaki. Rules for biologically inspired adaptive network design. *Science*, 327:439–442, 2010.

[34] S. Tsuda, M. Aono, and Y. P. Gunji. Robust and emergent *Physarum* logical-computing. *BioSystem*, 73:45–55, 2004.

[35] Ludwig Wittgenstein. *Tractatus Logico-Philosophicus.* Wilhelm Ostwald's Annalen der Naturphilosophie, 1922.

[36] 野矢茂樹. **『論理哲学論考』を読む**. 哲学書房, 2002.